To support this conclusion, we compared the rates of propene hydroformylation with the rates of *n*-butyrylcobalt tetracarbonyl isomerization at 2.5 bar and at 90 bar of P_{CO} (Table III). At 2.5 bar of P_{CO}, the rate of acyl isomerization is indeed higher than the rate of the overall aldehyde formation, and this makes an equilibration of the acyl isomers prior to the irreversible aldehyde formation conceivable under these conditions. At 90 bar of P_{CO}, however, the rate of acyl isomerization (because of its negative second order in CO) is 29 times slower than the rate of the aldehyde formation, and this severely hampers the isobutyrylcobalt tetracarbonyl formation from the primarily formed *n*-acyl isomer.

Finally, it should be mentioned that we have already repeatedly observed and described the consecutive isomerization of the kinetically favored acylcobalt carbonyl isomers formed from olefins and $CoH(CO)_4$ as primary products to the thermodynamically more stable isomers. In accord with our present findings, the olefins (styrene[22] or ethyl acrylate[23]) in those experiments were always present in excess with respect to the hydride.

Acknowledgment. We thank the Hungarian Academy of Sciences for financial support under Grant No. OTKA 2325 and Prof. J. F. Garst (Athens, GA) for discussions.

Registry No. 1, 38722-67-7; 2, 38784-32-6; CO, 630-08-0; $EtCOCo(CO)_4$, 16901-54-5; $HCo(CO)_4$, 16842-03-8; $PrCo(CO)_4$, 82687-61-4; ethene, 74-85-1; propene, 115-07-1; 1-heptene, 592-76-7.

(20) Natta, G.; Ercoli, R.; Castellano, S.; Barbieri, F. H. *J. Am. Chem. Soc.* **1954**, *76*, 4049.

(21) The steady-state concentration of octanoylcobalt tetracarbonyl at 80 °C has been reported as ca. 20% of the total cobalt on the basis of IR spectroscopic measurements of the band intensity at 2003 cm^{-1} using an ϵ_M value of 2740 M^{-1} cm^{-1}.[3] The ϵ_M value of the *n*-butyryl- and isobutyrylcobalt tetracarbonyls at 2004 and 2003 cm^{-1}, however, is 4950 and 4900 M^{-1} cm^{-1}, respectively,[9b] and therefore, 10% of the total cobalt in the form of acyl complexes under those conditions seems to be more realistic. The most recent ^{59}Co NMR spectrum revealed 4% of the total cobalt to be in the form of butyrylcobalt tetracarbonyl as the steady-state intermediate in propene hydroformylation at 80 °C.[4] We used this lowest value to calculate the actual acyl concentration in Table III.

(22) Ungváry, F.; Markó, L. *Organometallics* **1982**, *1*, 1120.

(23) Ungváry, F.; Markó, L. *Organometallics* **1986**, *5*, 2341.

Oxidative Addition of a P–O–P Linkage and Metal–Metal Bond Formation across a Dimolybdenum Cage

Haiying Yang and Edward H. Wong*

Department of Chemistry, University of New Hampshire, Durham, New Hampshire 03824

Jerry P. Jasinski, Roman Y. Pozdniakov, and Richard Woudenberg

Department of Chemistry, Keene State College, Keene, New Hampshire 03431

Received September 23, 1991

The dimolybdenum cage complex $Mo(CO)_4[^iPr_2NPO]_4Mo(CO)_4$ was reacted with tertiary phosphines of the type PPh_2R (R = Ph, Me, H) in refluxing toluene. In each case, incorporation of a single phosphine led to the loss of three carbonyls to form orange complexes of the type $Mo(CO)_3[^iPr_2NPO]_4Mo(CO)_2PPh_2R$ (**1a**, **1b**, **1c**). One- and two-dimensional ^{31}P NMR spectroscopy suggested substantial alterations of the parent adamantanoid cage structure upon CO replacement. By contrast, substitutions using trimethyl phosphite under milder conditions yielded both mono- and disubstituted products: $Mo(CO)_4[^iPr_2NPO]_4Mo(CO)_3P(OMe)_3$ (**2**) and $Mo(CO)_3P(OMe)_3[^iPr_2NPO]_4Mo(CO)_3P(OMe)_3$ (**3**) with the original core structure intact. The former can be shown by ^{31}P COSY NMR spectroscopy to be a mixture of *fac*- and *mer*-substituted diastereomers. The latter was found to be a mixture of all four disubstituted diastereomers. Upon further heating, both of these transformed to orange-red $Mo(CO)_3[^iPr_2NPO]_4Mo(CO)_2P(OMe)_3$ (**1d**) an analogue of complexes **1a**–**1c**. The X-ray molecular structure of **1d** has been determined. Crystal data: monoclinic, $P2_1/n$, a = 13.026 (3) Å, b = 21.054 (3) Å, c = 18.118 (3) Å, β = 103.46 (2)°, V = 4832 (2) Å^3, Z = 4, final R = 0.042, and R_w = 0.044 for 6070 reflections and varying 497 parameters. This revealed that a cage P–O–P bond has been cleaved near the substitution site with the resulting phosphinito oxygen replacing a second CO. Additionally, the phosphido group generated displaced a third CO at the other Mo center to bridge the two metals which are now within bonding distance (3.173 (1) Å) of each other. Similar reactions using pyridine also produced a related orange-red product, $Mo(CO)_3[^iPr_2NPO]_4Mo(CO)_2NC_5H_5$ (**1e**). This pyridine ligand is readily displaced by CO gas to generate $Mo(CO)_3[^iPr_2NPO]_4Mo(CO)_3$ (**1f**). The X-ray structure of **1f** has also been determined. Crystal data: monoclinic, $C2/c$, a = 36.523 (7) Å, b = 13.287 (5) Å, c = 20.348 (3) Å, β = 109.48 (1)°, V = 9310 (4) Å^3, Z = 8, final R = 0.055, and R_w = 0.074 for 4723 reflections and 452 variables. A similar polycyclic core structure to **1d** was found. Intermediates similar to **2** and **3** can be isolated in low yields from the PPh_2H reaction at below 100 °C.

Introduction

Nucleophilic substitution reactions at group VI metal carbonyls have been extensively studied.[1] For tetracarbonylmetal diphosphine chelate complexes, CO substitutions usually result in formation of either axial-substituted *mer*- or equatorial-substituted *fac*-$M(CO)_3P_3$ products.[2] The adamantanoid bimetallic cage complex $Mo(CO)_4[^iPr_2NPO]_4Mo(CO)_4$ (Figure 1) contains two mutually orthogonal $Mo(CO)_4P_2$ centers which are sub-

(1) For reviews, see: Wilkinson, G., Stone, F. G. A., Abel, E. W., Eds. *Comprehensive Organometallic Chemistry*, Pergamon: New York, 1982; Vol. 3, pp 795–806. Atwood, J. D. *Inorganic and Organometallic Reaction Mechanisms*; Brooks/Cole: Monterey, CA, 1985; pp 106–118. Howell, J. A. S.; Burkinshaw, P. M. *Chem. Rev.* **1983**, *83*, 557. Atwood, J. D.; Wovkulich, M. J.; Sonnenberger, D. C. *Acc. Chem. Res.* **1983**, *16*, 350. Poliakoff, M.; Weitz, E. *Adv. Organomet. Chem.* **1986**, *25*, 277.

* Address correspondence to this author.

0276-7333/92/2311-1579$03.00/0

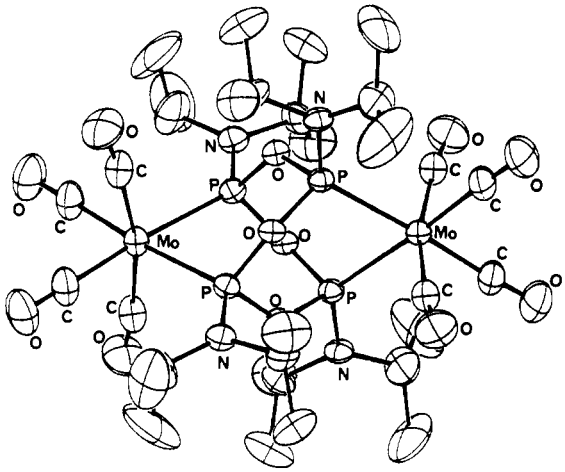

Figure 1. Molecular structure of the $Mo(CO)_4[^iPr_2NPO]_4Mo(CO)_4$ cage complex.

jected to considerable steric buttressing due to the rigid polycyclic structure.[3] Phosphine substituents at all four cage phosphorus vertices can influence each of the metal sites. For example, the trans CO–Mo–CO angle is compressed to only 167° due to diisopropylamino groups on the two remote P's. Halogenation reactions have already been shown to produce 16-electron trigonal prismatic $MoX_2(CO)_2P_2$ vertices, possibly as a result of this unique cage environment.[4] Nucleophilic substitutions at these centers may also generate unusual coordination chemistry due to similar constraints. We report here results from tertiary phosphine, phosphite, and pyridine substitutions at this cage complex. These revealed an unusual intramolecular P–O–P bond cleavage with extensive rearrangement of the core structure and formal oxidative addition to both metals, all direct consequences of the replacement of a carbonyl by a single phosphorus or nitrogen donor.

Results and Discussion

Substitution Reactions. Triphenylphosphine, diphenylmethylphosphine, and diphenylphosphine all reacted with the dimolybdenum cage complex $Mo(CO)_4[^iPr_2NPO]_4Mo(CO)_4$ in refluxing toluene to give orange-red products in moderate to good yields. Qualitatively, the reaction rates are in the order $PPh_3 < PPh_2Me < PPh_2H$. For example, after 4 h, spectral analyses indicated 40–50%, 60–70%, and over 90% conversion, respectively. These products (**1a**, **1b**, **1c** for $Mo(CO)_3[^iPr_2NPO]_4Mo(CO)_2L$

$$Mo(CO)_4[^iPr_2NPO]_4Mo(CO)_4 + L \rightarrow Mo(CO)_3[^iPr_2NPO]_4Mo(CO)_2L + 3CO$$

$$L = PPh_3\ (\mathbf{1a}),\ PPh_2Me\ (\mathbf{1b}),\ PPh_2H\ (\mathbf{1c})$$

with $L = PPh_3$, PPh_2Me, PPh_2H, respectively) can be isolated after routine column chromatography and recrystallization. In each case, spectral (vida infra) and elemental analyses revealed that while three CO's were lost, only a single phosphine was incorporated even in the presence of excess phosphine and prolonged reaction times. These data further suggested major disruptions in the basic cage structure.

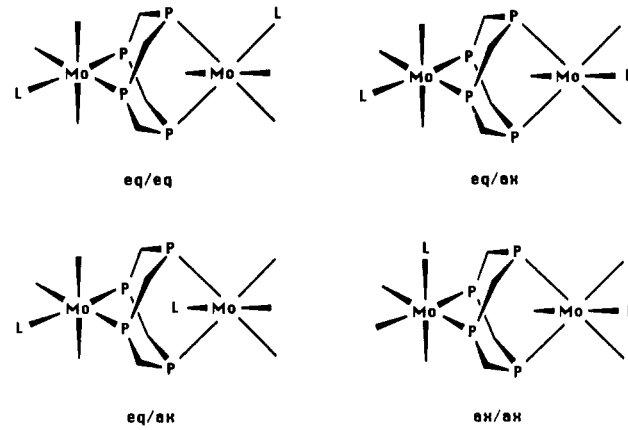

Figure 2. Four diastereomers for complex **3**, $Mo(CO)_3P(OMe)_3[^iPr_2NPO]_4Mo(CO)_3P(OMe)_3$: equatorial/equatorial, equatorial/axial-I, equatorial/axial-II, axial/axial.

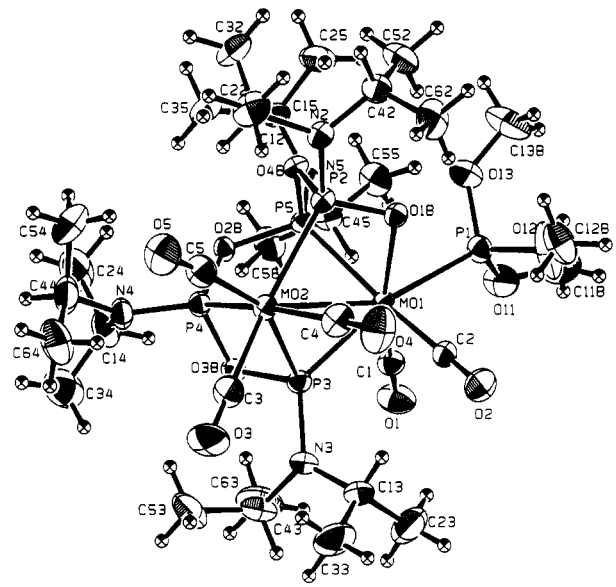

Figure 3. Molecular structure of complex **1d**, $Mo(CO)_3[^iPr_2NPO]Mo(CO)_2P(OMe)_3$.

By contrast, trimethyl phosphite reacted readily with the cage complex at 80–90 °C in toluene to give conventional mono- and disubstituted derivatives which can be separated by column chromatography. Spectral data suggested and HPLC confirmed the presence of all possible diastereomers (axial and equatorial for **2**; equatorial/

$$Mo(CO)_4[^iPr_2NPO]_4Mo(CO)_4 + P(OMe)_3 \rightarrow CO + Mo(CO)_4[^iPr_2NPO]_4Mo(CO)_3P(OMe)_3$$
2

$$2 + P(OMe)_3 \rightarrow Mo(CO)_3P(OMe)_3[^iPr_2NPO]_4Mo(CO)_3P(OMe)_3 + CO$$
3

equatorial, equatorial/axial (two types), and axial/axial for **3**, Figure 2) in both cases. Similar reaction conditions while the diphenylphosphines were used resulted in negligible cage reaction.

Upon refluxing in toluene, the colorless complexes **2** and **3** tranformed into orange-red $Mo(CO)_3[^iPr_2NPO]_4Mo$-

(2) Dobson, G. R.; Houk, L. W. *Inorg. Chim. Acta* **1967**, *1*, 287. Faber, G. C.; Dobson, G. R. *Inorg. Chim. Acta* **1968**, *2*, 479. Jenkins, J. M.; Moss, J. R.; Shaw, B. L. *J. Chem. Soc. A* **1969**, 2796. Dobson, G. R.; Rettenmaier, A. J. *Inorg. Chim. Acta* **1972**, *6*, 507. Isaacs, E. E.; Graham, W. A. G. *Inorg. Chem.* **1975**, *14*, 2560. Cohen, M. A.; Brown, T. L. *Inorg. Chem.* **1976**, *15*, 1417. Dobson, G. R.; Asali, K. A.; Marshall, J. L.; McDaniel, C. R., Jr. *J. Am. Chem. Soc.* **1977**, *99*, 8100. Dobson, G. R.; Asali, *Inorg. Chem.* **1981**, *20*, 3563. Darensbourg, D. J.; Zalewski, D. J.; Plepys, C.; Campana, C. *Inorg. Chem.* **1987**, *26*, 3727.

(3) Wong, E. H.; Turnbull, M. M.; Hutchinson, K. D.; Valdez, C.; Gabe, E. J.; Lee, F. L.; LePage, Y. *J. Am. Chem. Soc.* **1988**, *110*, 8422.

(4) Turnbull, M. M.; Valdez, C.; Wong, E. H.; Gabe, E. J.; Lee, F. L. *Inorg. Chem.* **1992**, *31*, 208.

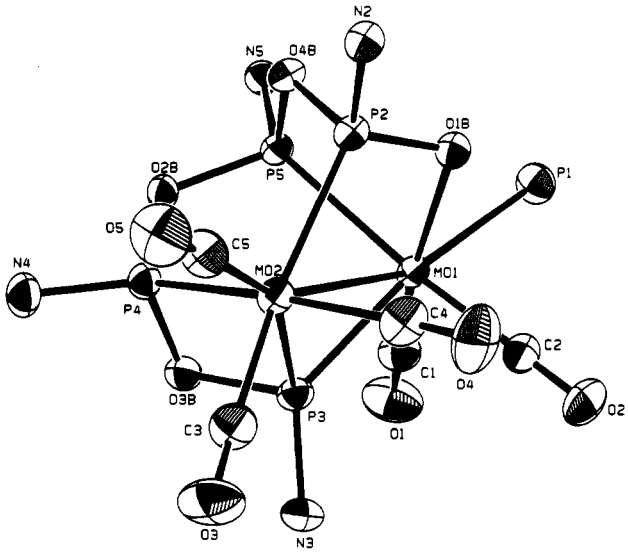

Figure 4. Core geometry of complex **1d**.

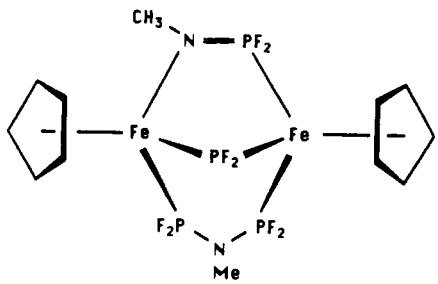

Figure 5. Structure of $[C_5H_5Fe(PF_2)_2NCH_3]_2$.[6]

$(CO)_2P(OMe)_3$ (**1d**), which is an analogue of complexes **1a–1c**.

$$\mathbf{2} \rightarrow \underset{\mathbf{1d}}{Mo(CO)_3[^iPr_2NPO]_4Mo(CO)_2P(OMe)_3} + 2CO$$

$$\mathbf{3} \rightarrow \mathbf{1d} + P(OMe)_3 + CO$$

A single-crystal X-ray diffraction study of **1d** (Figure 3) confirmed the loss of CO's and that one cage P–O–P bond has been cleaved with formation of one μ-P–O$^-$ and one μ-P$^-$ linking the two cage metals. The metals are now within bonding distance of each other at 3.173 (1) Å, a substantial contraction from the 6.001 (1) Å metal separation in the original cage. Complexes containing metals bridged simultaneously by a phosphido as well as a P–chalcogen group are known, though they are usually formed by insertion of chalcogens into a metal–phosphido bond.[5] King and co-worders have reported a P–N–P cleavage reaction in the photolysis of $CH_3N(PF_2)_2$ with $[CpFe(CO)_2]_2$.[6] The structure of the carbonyl-free product revealed a μ-PF_2NMePF_2 and a μ-PF_2 as well as a μ-PNMe group (Figure 5). This triple-bridging by three different ligands parallels that found in **1d**, though there is no accompanying metal–metal bond formation in this case.

A second phosphite ligand, the bulkier triphenyl phosphite, also yielded conventional substitution products similar to **2** and **3**. Traces of such products can also be observed in the reactions generating **1a–1c** when they are run under milder conditions. For example, workup and column chromatography of the cage/diphenylphosphine reaction after 72 h in refluxing hexane gave small amounts of the axial-substituted isomer **4** and diaxial-substituted isomer **5** (Figure 6). Both of these readily transformed to **1c** upon refluxing in toluene. It seems reasonable to postulate that simple substitution products were first formed in each case and are intermediates to the respective orange complexes **1a–1d**.

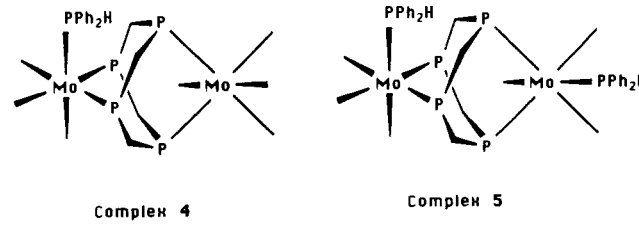

Figure 6. Complexes **4** and **5**.

Of the nitrogen nucleophiles tried, pyridine very readily afforded an orange complex **1e** analogous to **1a–1d**.

$$Mo(CO)_4[^iPr_2NPO]_4Mo(CO)_4 + NC_5H_5 \rightarrow \underset{\mathbf{1e}}{Mo(CO)_3[^iPr_2NPO]_4Mo(CO)_2NC_5H_5} + 3CO$$

Comparative substitution and transformation propensities can be gauged from reactions of the cage complex with the three diphenylphosphines, two phosphites, and pyridine under the same conditions. For example, after 4 h in refluxing toluene, the extent of depletion of starting material is in the order $P(OMe)_3 \approx$ pyridine > PPh_2H > $PPh_2Me \approx P(OPh)_3 > PPh_3$. Of the products formed, the proportion of orange complex versus simple substitution product decreases in the order pyridine > PPh_2H > PPh_2Me > $PPh_3 \approx P(OMe)_3 > P(OPh)_3$. These trends suggest a steric dependence on the entering ligand for the cage substitution step, while an electronic factor appears to be operating for the subsequent P–O–P cleavage and core rearrangement. Stronger π-acids like phosphites seem more reluctant to undergo this transformation. This is especially true for the small trimethyl phosphite ligand (cone angle 107°) whose substitution reaction was essentially complete within 4 h with orange **1d** present only as a minor product. By contrast, pyridine, the least π-acidic of the five, completely converted the cage to orange **1e** within this same time period.

Secondary amines like piperidine and diisopropylamine degraded the cage complex to give *bis*(dialkylamino)-phosphine oxides.[3]

$$Mo(CO)_4[^iPr_2NPO]_4Mo(CO)_4 + HNC_5H_{10}\ (\text{excess}) \rightarrow (^iPr_2N)_2P(O)H + (^iPr_2N)(C_5H_{10}N)P(O)H + (C_5H_{10}N)_2P(O)H + Mo(CO)_4(HN_5H_{10})_2 + \text{etc.}$$

Both transamination and nucleophilic P–O–P cleavage have occurred, resulting in essentially a reversal of the cage formation reaction from $Mo(CO)_6$ and $(^iPr_2N)_2P(O)H$.[3]

The pyridine in complex **1e** is readily replaced by CO gas to yield $Mo(CO)_3[^iPr_2NPO]_4Mo(CO)_3$ (**1f**), whose molecular structure has been determined (Figure 7). Both **1e** and **1f** are suitable precursors for the synthesis of **1a–1d** by reaction with the appropriate phosphorus ligand.

Molecular Structure of 1d. The molecular structure of complex **1d** is shown in Figures 3 and 4. Extensive alterations in the metal coordination spheres and cage geometry are evident. One P–O–P bond has been cleaved, while a total of three carbonyls have been lost upon adducting of the trimethyl phosphite. At Mo(1), one carbonyl has been substituted by this ligand while a second was displaced by the phosphinito oxygen (P(2)–O(1B)) from the cleaved P–O–P linkage. The resulting aminophosphido group at P(3) further dislodged another carbonyl from Mo(2) and now bridges the two metal centers, thereby forming a four-membered Mo(2)–P(3)–O(3B)–P(4) chelate

(5) Klingert, B.; Werner, H. *J. Organomet. Chem.* **1983**, *252*, C47.
(6) Newton, M. G.; King, R. B.; Chang, M.; Gimeno, J. *J. Am. Chem. Soc.* **1978**, *100*, 1632.

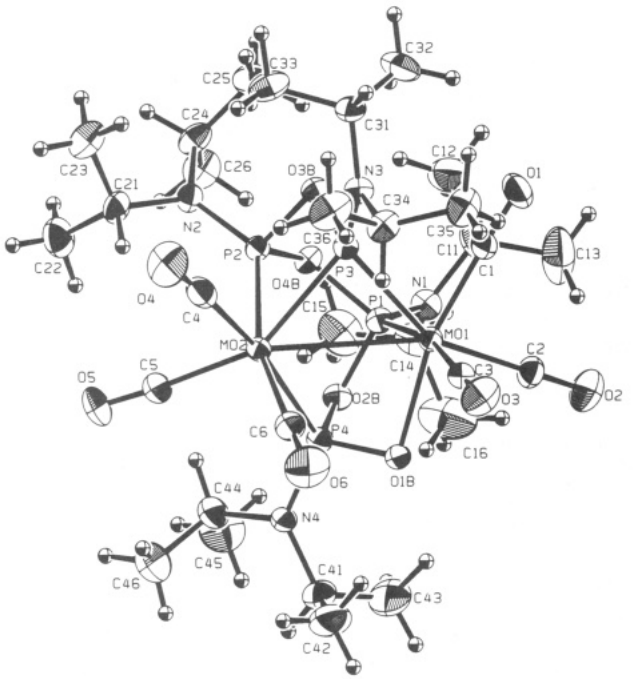

Figure 7. Molecular structure of complex **1f**, $Mo(CO)_3$-$[^iPr_2NPO]_4Mo(CO)_3$.

ring. The Mo(1)–Mo(2) separation is 3.173 (1) Å. This contrasts strikingly with the 6.001 (1) Å Mo···Mo separation found in the parent cage structure. Molybdenum–molybdenum single-bond distances vary depending on ligand constraints, and 3.173 (1) Å is well within the 3.057 (6)–3.235 (1)-Å range of weak single bonds reported for $Mo_2(CO)_8(\mu\text{-}PEt_2)_2$ and $Cp_2Mo_2(CO)_6$, respectively.[7] Electron counting also requires the presence of a single Mo–Mo bond to achieve the noble-gas configuration at both Mo(1) and Mo(2) if we assign them both +1 formal oxidation states.

A short metal–phosphorus distance of 2.353 (2) Å is found for Mo(1)–P(3) which is approximately trans to the $P(OMe)_3$ ligand. All other Mo–P bonds are in the range 2.46–2.53 Å, not significantly changed from the value of 2.50 Å in the parent cage complex. Mo(1)–O(1B) is at 2.226 (3) Å, with the trans Mo(1)–C(1) bond length of 1.952 (6) Å marginally shorter than all other Mo–C bonds within the structure (1.97–2.00 Å). Except at P(2), ring P–O distances range from 1.60 to 1.67 Å. The two disparate P(2)–O distances with P(2)–O(1B) at 1.537 (3) Å and P(2)–O(4B) at 1.730 (3) Å reflect considerable multiple-bond character in the former at the expense of the latter. Corbridge has summarized bond length data for phosphates to find an average of 1.54 Å for the reported P–O distances.[8]

Though both coordination spheres approximate an octahedron, substantial deviations from idealized angles are found due to the polycyclic ligand system bridging the two metals. At Mo(2), the four-membered M–P–O–P chelate ring compresses the P(3)–Mo(2)–P(4) angle to only 62.33 (5)°.[9] Furthermore, the five-membered Mo(1)–P(3)–Mo(2)–P(2)–O(1B) heterocycle contains a narrow Mo(1)–P(2)–Mo(2) μ-phosphido angle of 82.02 (5)° while the P(3)–Mo(1)–O(1B) angle is distended to 124.7 (1)°. As a result, the angle closest to linearity at Mo(1) is P(5)–Mo(1)–C(2) at only 168.7 (2)°. The four equatorial ligand atoms P(1), P(3), O(1B), and C(1) then subtend very distorted angles at Mo(1); P(3)–Mo(1)–O(1B) is 124.7 (1)°, P(3)–Mo(1)–C(1) is 72.9 (2)°, C(1)–Mo(1)–P(1) is 83.1 (2)°, and P(1)–Mo(1)–O(1B) is 79.3 (1)°. However, these equatorial angles do sum up to 360°. At Mo(2), P(2) and C(3) are approximately axial (P(2)–Mo(2)–C(3) is 171.0 (2)°). The corresponding equatorial angles deviate widely from orthogonality ranging from 62.3 to 102.6° but summing up to 361°.

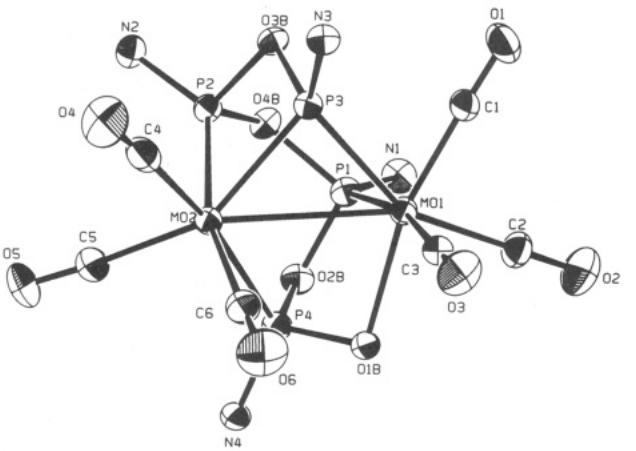

Figure 8. Core geometry of complex **1f**.

Table I. Infrared Absorptions for the Complexes[a]

	CO region, cm^{-1}	POP region, cm^{-1}
1a	1977, 1925, 1904, 1884, 1854	870, 849, 832, 800
1b	1975, 1917, 1896, 1853	875, 845, 805
1c	1977, 1921, 1895, 1856	874, 856, 826, 805
1d	1979, 1925, 1889, 1856	870, 843, 834, 800
1e	1973, 1915, 1889, 1874, 1851	875, 839, 800
1f	2011, 1983, 1944, 1921, 1917, 1909, 1903, 1893	877, 847, 810
2	2003, 1988, 1975, 1937, 1916, 1900 (sh), 1887	866, 845
3	1985, 1965, 1920 (sh), 1877 (bd), 1860 (sh)	867, 846
4	2013, 1962, 1941, 1927, 1905, 1886, 1861	864, 832
5	1952, 1860	864, 833

[a] KBr disks.

Molecular Structure of 1f. The molecular geometry of complex **1f** is shown in Figures 7 and 8. A similar polycyclic structure to **1d** is found. The replacement of a trimethyl phosphite by a CO generated relatively few alterations in bonding details. The Mo(1)–Mo(2) bond is now at 3.143 (1) Å. a lengthening of the Mo(1)–P(3) bond from 2.353 (2) to 2.403 (3) Å is observed with a CO instead of the $P(OMe)_3$ trans to it. The Mo(1)–O(1B) bond is unchanged from **1d** at 2.265 (7) Å, while the metal–carbonyl bond trans to it (Mo(1)–C(1)) is clearly the shortest at 1.94 (1) Å compared to the other Mo–C bonds ranging from 2.01 to 2.11 Å. Again, a short P(4)–O(1B) at 1.526 (7) Å and long P(4)–O(2B) at 1.742 (8) Å result from preferential multiple bonding to O(1B).

Bond angles and coordination geometry around Mo(2) are similar to those in **1d**. With the substitution of a phosphite by a CO, more substantial changes are observed at Mo(1). For example, C(3) now subtends reasonably orthogonal angles at Mo(1), with C(1), C(2), O(1B), and P(3) ranging from 88.9 (4) to 94.8 (5)°. In **1d**, the corresponding angles from P(1) are in the range 79.3 (1)–93.20 (5)°. trans ligands closest to linearity at Mo(1) are P(1) with C(3), giving a P(1)–Mo(1)–C(3) angle of 167.7 (3)°, while at Mo(2) P(4)–Mo(2)–C(4) has a value of 168.7 (4)°.

(7) Dahl, L.; Rudulfo de Gil, E.; Feltham, R. D. *J. Am. Chem. Soc.* **1969**, *91*, 1653. Adams, R. D.; Collins, D. M.; Cotton, F. A. *Inorg. Chem.* **1974**, *13*, 1086. Nassimbeni, L. R. *Inorg. Nucl. Chem. Lett.* **1971**, *7*, 909. Mais, R. H. B.; Owston, P. G.; Thompson, D. T. *J. Chem. Soc. A* **1967**, 1735.

(8) Corbridge, D. E. C. *Phosphorus: An Outline of its Chemistry, Biochemistry, and Technology*, 3rd ed.; Elsevier: Amsterdam, 1985; Chapter 1.

(9) Wong, E. H.; Prasad, L.; Gabe, E. J.; Bradley, F. C. *J. Organomet. Chem.* **1982**, *236*, 321.

Both the four-membered Mo(2)–P(2)–O(3B)–P(3) and five-membered Mo(1)–O(1B)–P(4)–Mo(2)–P(3) rings are essentially unchanged from their counterparts in **1d**. Likewise, the phosphido Mo(1)–P(3)–Mo(2) angle is only slightly compressed to 80.9 (1)° in accord with the decreased Mo–Mo distance.

Infrared Spectra. The orange complexes **1a–1e** all exhibit metal carbonyl stretches below 2000 cm^{-1}, with four to five well-resolved bands between 1850 and 1980 cm^{-1} (Table I) indicative of low overall symmetry. These values also suggest that the cis-$Mo(CO)_4P_2$ coordination sphere at the unsubstituted metal site is no longer intact. Complex **1f** has a band at 2011 cm^{-1} as well as numerous bands between 1890 and 2000 cm^{-1}. As mixtures of diastereomers, complex **2** exhibits six resolved bands as well as a shoulder at 1900 cm^{-1} while complex **3** has only three resolved bands at 1877, 1965, and 1985 cm^{-1} with broad shoulders at 1920 as well as 1860 cm^{-1}. Complex **5** exhibits only two CO stretches at 1952 and 1860 cm^{-1}, consistent with a *fac*-CO arrangement. Broad POP bands in the 800–880-cm^{-1} region are also common to all these products.[10] Additionally, a broad, medium-intensity P–O band at 1105 cm^{-1} is noted for each of **1a–1f**.

^{31}P NMR Spectra. Proton-decoupled ^{31}P NMR data for the described complexes are presented in Table II. The D_{2d} symmetry of the cage molecule is completely lost upon formation of complexes **1a–1d** since in each case five separate resonances can be seen in their ^{31}P NMR spectra. Significantly, a low-field multiplet at around 305–307 ppm is observed in each case, independent of the nature of the entering nucleophile. This chemical shift is inconsistent with typical Mo-coordinated tertiary phosphines or phosphites and is instead in the region for phosphenium cations or phosphido ligands.[11,12] The X-ray structures of **1d** and **1f** explicitly showed the latter to be present. Since the phosphido chemical shift is known to be quite sensitive to the M–P–M angle and the extent of metal–metal interaction,[13] the nearly invariant shift value at around +306 ppm implies that this particular angle as well as the nature of metal–metal bonding remain little changed through the series **1a–1d**. This is also borne out by the solid-state structural data of **1d** and **1f**. The highest-field resonance due to the newly-coordinated phosphine ligands in **1a–1c** can be readily assigned using typical coordination shifts from the free ligand value.[14] In the case of **1c**, a proton-coupled spectrum clearly identifies the high-field multiplet as the PPh_2H resonance with a $^1J_{P-H}$ of 334 Hz. Connectivity between the five resonances in each complex can be unambiguously established by ^{31}P COSY spectroscopy. Resolved P–P coupling constants are in the range 10–130 Hz.

Conventional ^{31}P NMR spectra of complex **2** suggested a mixture of isomers. A 2-D COSY spectrum readily allowed identification of its composition as being 40% axial-substituted and 60% equatorial-substituted $Mo(CO)_4[^iPr_2NPO]_4Mo(CO)_3P(OMe)_3$ isomers (see supplementary data). Similarly, the extremely complex 1-D spectrum of **3** can be satisfactorily resolved into its four diastereomeric components by its 2-D COSY spectrum (supplementary data). The relative proportions of the equatorial/equatorial, equatorial/axial (two types), and axial/axial isomers are approximately 2:1:1:1, again indicating a preference for equatorial substitution.

Table II. ^{31}P Data for the Complexes

complexes		chem shift δ, ppm (J, Hz)
1a	AJMNX	δ_A = 307.5, δ_J = 156.9, δ_M = 124.3, δ_N = 123.3, δ_X = 24.9 ($J_{AJ} = J_{AN}$ = 14.7, J_{AM} = 19.1, J_{AX} = 49.8, J_{JM} = 77.7, J_{JN} = 126.0, J_{JX} = 24.9, J_{MN} = 36.7)
1b	AJMNX	δ_A = 305.5, δ_J = 156.9, δ_M = 129.3, δ_N = 125.4, δ_X = 15.3 (J_{AJ} = 14.7, J_{AM} = 17.6, J_{AN} = 11.7, J_{AX} = 52.8, J_{JM} = 79.1, J_{JN} = 129.0, J_{JX} = 26.4, J_{MN} = 38.1)
1c	AJMNX	δ_A = 305.9, δ_J = 154.9, δ_M = 128.8, δ_N = 127.1, δ_X = 23.3 ($J_{AJ} = J_{AM}$ = 14.7, J_{AN} = 11.7, J_{AX} = 52.8, J_{JM} = 90.9, J_{JN} = 129.0, J_{JX} = 29.3, J_{MN} = 38.1)
1d	AMNXY	δ_A = 306.8, δ_M = 153.7, δ_N = 149.8, δ_X = 129.7, δ_Y = 123.9 (J_{XY} = 38.1, other J's not obtained)
1e	AMXY	δ_A = 295.3, δ_M = 150.7, δ_X = 134.7, δ_Y = 128.1 (J_{AM} = 14.7, J_{AX} = 12.2, J_{AY} = 17.1, J_{MX} = 125.7, J_{MY} = 80.6, J_{XY} = 36.6)
1f	AXYZ	δ_A = 306.3, δ_X = 149.8, δ_Y = 131.6, δ_Z = 121.4 (J_{AX} = 15.4, J_{AY} = 24.2, J_{AZ} = 11.0, J_{XY} = 101.1, J_{XZ} = 127.4, J_{XY} = 37.4)
2	$AMNX_2$	δ_A = 180.0, δ_M = 164.0, δ_N = 155.6, δ_X = 148.2 (J_{AM} = 187.1, J_{AN} = 41.0, J_{MN} = 47.5, J_{MX} = 10.5, J_{NX} = 6.7)
	AM_2NX	δ_A = 166.9, δ_M = 155.0, δ_N = 151.2, δ_X = 148.2 (J_{AM} = 45.1, J_{MN} = 10.5, J_{MX} = 6.7, J_{NX} = 48.3)
3	AMX	δ_A = 179.3, δ_M = 159.8, δ_X = 151.6 (J_{AM} = 185.5, J_{AX} = 40.9, J_{MX} = 51.1 Hz)
	$AMNX_2Y$	δ_A = 178.6, δ_M = 164.7, δ_N = 158.8, δ_X and $\delta_Y \approx$ 151.6 (J_{AN} = 187.1, other J's not obtained)
	$AMNX_2Y$	δ_A = 178.1, δ_M = 163.8, δ_N = 162.0, δ_X and $\delta_Y \approx$ 153.5 (J_{AN} = 190.0, other J's not obtained)
	AXY	δ_A = 165.8, δ_X and $\delta_Y \approx$ 151.6 (J's not obtained)
4	A_2M_2X	δ_A = 157.1, δ_M = 149.6, δ_X = 12.9 (J_{AM} = 7.0, J_{AX} = 32.8, J_{MX} = 0)
5	A_2X	δ_A = 157.3, δ_X = 13.5 (J_{AX} = 34.2)

Complex **4** exhibits an A_2M_2X spectrum consistent with substitution of an axial CO by PPh_2H and a C_s molecular symmetry. This requires that the two remote P resonances remain magnetically equivalent in spite of the asymmetry introduced at the substituted molybdenum. Complex **5** gives a first-order A_2X pattern indicating little or no P–O–P coupling across the cage.

^{1}H and ^{13}C NMR Spectra. Proton and carbon-13 NMR data of the complexes are listed in the Experimental Section. The metal carbonyl resonances are especially useful in assisting several structural assignments. For example, complex **1d** exhibited four distinct groups of multiplets between δ 218 and 223 ppm while **1f** displayed five separate CO multiplets (δ 207–221 ppm), in agreement with the low molecular symmetry found in both solid-state structures.

Conclusions

Carbonyl substitution at the molybdenum cage complex using triphenyl-, diphenylmethyl-, and diphenylphosphines or pyridine resulted in net addition of one ligand and loss of three carbonyls. One P–O–P intracage linkage has been cleaved and oxidatively added to the two molybdenum

(10) Corbridge, D. E. C. *Top. Phosphorus Chem.* **1969**, *6*, 235. Wong, E. H.; Ravenelle, R.; Gabe, E. J.; Lee, F. L.; Prasad, L. *J. Organomet. Chem.* **1982**, *233*, 321.

(11) Verkade, J. G.; Quin, L. D. *P-31 NMR Spectroscopy in Stereochemical Analysis*; VCH: New York, 1987; Chapter 16.

(12) Verkade, J. G.; Quin, L. D. *P-31 NMR Spectroscopy in Stereochemical Analysis*; VCH: New York, 1987; Chapter 17.

(13) Petersen, J. L.; Stewart, R. P. *Inorg. Chem.* **1980**, *19*, 186. Carty, A. J.; MacLaughlin, S. A.; Taylor, N. J. *J. Organomet. Chem.* **1981**, *204*, C27.

(14) Pregosin, P. S.; Kunz, R. W. *^{31}P and ^{13}C NMR of Transition Metal Phosphine Complexes*; Springer-Verlag: Berlin, 1979.

Scheme I

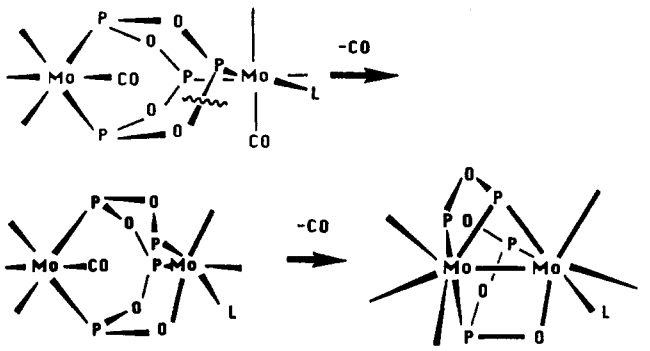

vertices to create a μ_2-PO^- as well as a μ_2-P^- bridge. In addition, an intracage metal–metal bond has formed (Scheme I). The facility for this transformation appears to depend on the π-acceptor strength of the adducted nucleophile since conventional mono- and disubstituted complexes can be obtained using π-acidic phosphites. Upon further heating, these substitution products undergo similar intramolecular transformations to give analogues of the phosphine and pyridine adducts.

Experimental Section

All manipulations were carried out using standard Schlenk techniques under an atmosphere of prepurified nitrogen. Hexane and methylene chloride were distilled from CaH_2, and toluene was distilled from sodium metal. The phosphines were used as purchased from Strem Chemicals. Pyridine, diisopropylamine, piperidine, ethyl acetate, and acetonitrile were reagent grade obtained from Aldrich Chemicals. Alumina (Aldrich Chemicals, Brockmann I, neutral) was used as received. The cage complex was synthesized as described previously.[3] ^1H, ^{13}C, and ^{31}P NMR spectra were recorded on JEOL FX90Q and Bruker AM360 spectromers using an internal deuterium lock. Unless otherwise noted, all spectra were run in $CDCl_3$. ^1H and ^{13}C chemical shifts were referenced to internal TMS, while ^{31}P shifts were referenced to external 85% phosphoric acid. Infrared spectra were recorded on a Perkin-Elmer 283B instrument. Elemental analyses were performed at the University Instrumentation Center using a Perkin-Elmer 240b elemental analyzer.

$Mo(CO)_3[^iPr_2NPO]_4Mo(CO)_2PPh_3$ (1a). A 25-mL round-bottomed flask was charged with 1.00 g (1.00 mmol) of the cage complex, 0.52 g (2.0 mmol) of triphenylphosphine, a magnetic stirbar, and 10 mL of toluene. After refluxing for 24 h, the clear, red solution was evaporated to dryness under reduced pressure. A 15-mL aliquot of hexane was added to extract the residue. The extract was stripped onto alumina and chromatographed on a 1- × 30-cm column of alumina using 2% ethyl acetate in hexane as eluant. Complex **1a** was obtained as an orange-red band in 40% yield (0.47 g). Analytical samples were obtained by slow evaporation from hexane. ^1H NMR: δ 7.86 and 7.24 (m, Ph), 3.86 and 3.68 (m, N–CH), 1.33, 1.32, 1.30, 1.20, 1.19, 1.13, 1.02, 0.87 (d, CH_3, J = 6.7–6.8 Hz). ^{13}C NMR: δ 222.7 and 221.7 (m, CO), 218.4 (dd, CO, J = 18.8, 54.2 Hz), 137.0–128.1 (m, Ph), 49.1, 48.6, 46.4, 44.8 (d, N–C, J = 12.4, 7.5, 9.3, 8.6 Hz), 23.3 (m, Me). Anal. Calcd for $C_{47}H_{71}Mo_2N_4O_9P_5$: C, 47.72; H, 6.05; N, 4.74. Found: C, 47.79; H, 6.15; N, 4.68.

$Mo(CO)_3[^iPr_2NPO]_4Mo(CO)_2PPh_2R$ (1b, R = Me; 1c, R = H). A 25-mL round-bottomed flask was charged with a stirbar, 1.00 g (1.00 mmol) of the cage complex, 10 mL of toluene, and 2.00 mmol of the respective phosphine. After refluxing for 24 h, the clear red solutions were stripped of the toluene under reduced pressure. Upon standing for 1 day, the resulting viscous oils afforded red crystals of the products. These were washed with small portions of cold hexane and dried to give an 80% yield of **1b** or **1c**. ^1H NMR (for **1b**): δ 7.75–7.30 (m, Ph), 3.97 and 3.70 (m, N–CH), 2.02, 1.45, 1.36, 1.28, 1.23, 1.20 (d, Me, J = 8.3, 6.7, 6.7, 7.7, 6.9, 6.8 Hz). ^1H NMR (for **1c**): δ 7.77–7.32 (m, Ph), 6.51 (dd, P–H, J = 9, 332 Hz), 4.0–3.55 (m, NCH), 1.49, 1.32, 1.27, 1.10, 1.00 (d, J = 6.7–6.8 Hz). ^{13}C NMR (for **1b**): δ 224.9 and 221.1 (m, CO), 218.6 (dd, CO, J = 14.6, 36.4 Hz), 138–127.9 (m, Ph), 48.43, 48.38, 46.2, 44.8 (d, N–C, J = 7.5, 10.0, 8.7, 8.7 Hz), 24.5 (s, Me), 23.3 (m, Me), 15.3 (d, Me, J = 19.3 Hz). ^{13}C NMR (for **1c**): δ 223.2 and 221.2 (m, CO), 218.2 (dd, J = 15.2, 51.3 Hz), 134.2–128.7 (m, Ph), 48.5, 47.9, 46.5, 44.5 (d, NC, J = 8.4, 9.2, 9.2, 8.5 Hz), 24.5 (d, Me, J = 7.8 Hz), 22.9 (m, Me). Anal. Calcd for $C_{42}H_{69}Mo_2N_4O_9P_5$ (**1b**): C, 45.01; H, 6.20; N, 4.60. Found: C, 45.18; H, 6.27; N, 5.00. Calcd for $C_{41}H_{67}Mo_2N_4O_9P_5$ (**1c**): C, 44.49; H, 6.10; N, 5.06. Found: C, 44.34; H, 6.48; N, 4.72.

$Mo(CO)_4[^iPr_2NPO]_4Mo(CO)_3PPh_2H$ (4) and $Mo(CO)_3PPh_2H[^iPr_2NPO]_4Mo(CO)_3PPh_2H$ (5). A 25-mL round-bottomed flask was charged with a stirbar, 0.20 g (0.20 mmol) of the cage complex, 10 mL of hexane, and 2.0 mmol of the diphenylphosphine. After refluxing for 3 days, TLC indicated four spots. The light-yellow solution was evaporated under reduced pressure and the residue chromatographed on an alumina column as described for **1a**. The second complex to elute was complex **4** isolated in 11% yield (25 mg), and the fourth was complex **5** isolated in 4% yield (10 mg). ^1H NMR (for **4** in C_6D_6): δ 7.60 and 7.05 (m, Ph), 6.39 (d of t, P–H, J = 4.2, 309.7 Hz), 4.78 (septet, N–CH, J = 6.4 Hz), 4.55 and 4.11 (m, N–CH), 1.36 (m, Me), 1.04 (d, Me, J = 7.0 Hz). ^{13}C NMR (for **4** in C_6D_6): δ 217.7, 217.1, 214.9 (m, CO), 135.0–128.8 (m, Ph), 47.4 (m, N–C), 25.6, 24.3, 23.9 (m, Me). ^1H NMR (for **5** in C_6D_6): δ 7.70 and 7.05 (m, Ph), 6.43 (d, P–H, J = 304.9 Hz), 4.93 and 4.54 (m, N–CH), 1.46, 1.45, 1.15, 1.07 (d, Me, J = 6.9, 7.0, 7.1, 6.9). ^{13}C NMR (for **5** in C_6D_6): δ 218.0 (m, CO), 136.1–128.8 (m, Ph), 47.5 (m, N–C), 25.7–24.2 (m, Me). Anal. Calcd for $C_{43}H_{67}Mo_2N_4O_{11}P_5$ (**4**): C, 44.42; H, 5.81; N, 4.82. Found: C, 44.19; H, 5.83; N, 4.53. Calcd for $C_{54}H_{78}Mo_2O_{10}P_6$ (**5**): C, 49.10; H, 5.95; N, 4.38. Found: C, 47.36; H, 6.38; N, 4.24. Due to the very low yields of **5**, repeated efforts failed to improve on these elemental data.

$Mo(CO)_4[^iPr_2NPO]_4Mo(CO)_3P(OMe)_3$ (2) and $Mo(CO)_3P(OMe)_3[^iPr_2NPO]_4Mo(CO)_3P(OMe)_3$ (3). A 25-mL round-bottomed flask containing a stirbar, 1.00 g (1.00 mmol of cage complex, and 0.25 mL (2.1 mmol) of $P(OMe)_3$ was refluxed for 6 h. The clear yellow solution was evaporated under reduced pressure and the light-yellow residue chromatographed on an alumina column as for **1a**. An amount of 0.34 g (0.32 mmol, 32% yield based on cage) of complex **2** was obtained followed by 0.60 g (0.50 mmol, 50% yield based on cage) of complex **3**. ^1H NMR (for **2**): δ 4.57 and 4.38 (unresolved multiplets, N–CH), 3.61 and 3.59 (d, OMe, J = 11.2, 10.4 Hz), 1.3–1.5 (overlapping doublets, Me). ^{13}C NMR (for **2**): δ 217.4, 213.6, 210.3, 206.6 (unresolved multiplets, CO), 50.2, 46.0 (unresolved multiplets, N–CH and OMe), 23.5 (unresolved multiplet, Me). ^1H NMR (for **3**): δ 4.66 and 4.53 (unresolved multiplet, N–CH), ~3.6 (unresolved multiplet, OMe), ~1.35 (overlapping doublets, Me). ^{13}C NMR (for **3**): δ 219.3, 217.8, 214.3, 211.7 (unresolved multiplets, CO), 51.2 and 46.7 (unresolved multiplets, NC, OMe), 24.7 (unresolved multiplet, Me). Anal. Calcd for $C_{34}H_{65}Mo_2N_4O_{14}P_5$ (**2**): C, 37.10; H, 5.95; N, 5.09. Found: C, 36.99; H, 6.08; N, 4.96. Calcd for $C_{36}H_{74}Mo_2N_4O_{16}P_6$ (**3**): C, 36.13; H, 6.23; N, 4.68. Found: C, 36.11; H, 6.12; N, 4.72.

$Mo(CO)_3[^iPr_2NPO]_4Mo(CO)_2P(OMe)_3$ (1d). The same procedure for the syntheses of complexes **2** and **3** was followed except that the reaction mixture was refluxed for 34 h. After chromatography, 0.72 g (0.69 mmol, 69% yield) of **1d** was obtained. X-ray-quality crystals were obtained by slow evaporation from a hexane solution. ^1H NMR (C_6D_6): δ 4.02, 3.80, 3.65 (m, NCH), 3.60 (d, OMe, J = 10.6 Hz), 1.47 and 1.32 (d, Me, J = 6.7 and 6.8 Hz), 1.39 and 1.21 (m, Me). ^{13}C NMR (C_6D_6): δ 223.2, 221.8, 220.2 (m, CO), 218.6 (dd, CO, J = 15.6, 50.6 Hz), 52.2, 48.4, 48.1, 46.5, 44.6 (d, NC or OMe, J = 5.2, 8.4, 10.6, 9.4, 8.4 Hz), 23.0, 22.7, 22.6, 22.3 (m, Me). Anal. Calcd for $C_{32}H_{65}Mo_2N_4O_{12}P_5$ (**1d**): C, 36.79; H, 6.27; N, 5.36. Found: C, 36.71; H, 6.58; N, 5.00.

$Mo(CO)_3[^iPr_2NPO]_4Mo(CO)_2NC_6H_5$ (1e). A reaction mixture of 2.00 g of cage complex, 2.00 mL (23.9 mmol) of pyridine, and 18 mL of toluene were refluxed for about 9 h. The deep red solution was filtered to remove some brown precipitate. The filtrate was evaporated to dryness under reduced pressure and the residue washed with several portions of hexane to give 1.52 g (1.52 mmol, 76% yield) of complex **1e**. ^1H NMR: δ 9.11–7.29 (m, Py), 4.03, 3.85, 3.71, 3.44 (septets, NCH, J = 6.6, 6.8, 6.9, 6.7 Hz), 1.51, 1.47, 1.41, 1.38, 1.29, 1.26, 1.19 (d, Me, J = 6.7, 6.7, 6.8, 6.8, 6.9, 6.9, 6.8 Hz). ^{13}C NMR δ 228.1 (dd, CO, J = 12.1, 44.0 Hz), 221.4 and 218.2 (m, CO), 153.4–124.2 (m, Py), 48.4, 47.5, 46.5,

Table III. Crystal Data for Complexes 1d and 1f

	1d	1f
formula	$Mo_2P_5O_{12}N_4C_{32}H_{65}$	$Mo_2P_4N_4O_{10}C_{30}H_{56}$
fw	1044.63	948.57
space group	$P2_1/n$ monoclinic	$C2/c$ monoclinic
a, Å	13.026 (3)	36.523 (7)
b, Å	21.054 (3)	13.287 (5)
c, Å	18.118 (3)	20.348 (3)
β, deg	103.46 (2)	109.48 (1)
Z	4	8
d_{calc}, g cm^{-1}	1.436	1.353
μ, mm^{-1}	7.22	7.07
cryst dimens, mm	0.6 × 0.4 × 0.7	1.0 × 1.0 × 1.0
λ(Mo Kα radiation), Å	0.71069	0.71069
data collcd	$0° < 2\theta < 55.0°$	$0° < 2\theta < 55.0°$
scan	ω	ω
no. of unique reflcns	11384	11325
no. of obsd reflcns	6070	4770
$F(000)$	2160	3904
R_F	0.042	0.054
R_{wF}	0.044	0.074
GOF	1.32	2.00

Table IV. Selected Bond Distances (Å) and Angles (deg) for 1d[a]

Mo(1)-Mo(2)	3.173 (1)		
Mo(1)-P(1)	2.465 (2)	P(2)-O(1B)	1.537 (3)
Mo(1)-P(3)	2.353 (2)	P(2)-O(4B)	1.730 (3)
Mo(1)-P(5)	2.532 (1)	P(3)-O(3B)	1.654 (4)
Mo(1)-O(1B)	2.226 (3)	P(4)-O(2B)	1.626 (3)
Mo(1)-C(1)	1.952 (6)	P(3)-O(3B)	1.662 (3)
Mo(1)-C(2)	1.969 (6)	P(5)-O(2B)	1.670 (3)
Mo(2)-P(2)	2.525 (2)	P(5)-O(4B)	1.604 (3)
Mo(2)-P(3)	2.480 (2)	C(1)-O(1)	1.157 (6)
Mo(2)-P(4)	2.486 (2)	C(2)-O(2)	1.159 (6)
Mo(2)-C(3)	1.964 (6)	C(3)-O(3)	1.150 (7)
Mo(2)-C(4)	2.005 (7)	C(4)-O(4)	1.141 (7)
Mo(2)-C(5)	1.993 (7)	C(5)-O(5)	1.151 (7)
Mo(2)-Mo(1)-P(1)	153.12 (4)	Mo(1)-Mo(2)-P(2)	60.08 (3)
Mo(2)-Mo(1)-P(2)	48.83 (3)	Mo(1)-Mo(2)-P(3)	47.25 (3)
Mo(2)-Mo(1)-P(3)	50.73 (4)	Mo(1)-Mo(2)-P(4)	81.01 (4)
Mo(2)-Mo(1)-P(5)	78.46 (3)	Mo(2)-Mo(1)-O(1B)	74.01 (9)
P(1)-Mo(1)-P(3)	155.97 (5)	P(2)-Mo(2)-P(3)	105.10 (5)
P(1)-Mo(1)-P(5)	93.20 (5)	P(2)-Mo(2)-P(4)	93.95 (5)
P(1)-Mo(1)-O(1B)	79.30 (9)	P(2)-Mo(2)-C(3)	171.0 (2)
P(1)-Mo(1)-C(1)	83.1 (2)	P(2)-Mo(2)-C(4)	84.3 (2)
P(1)-Mo(1)-C(2)	88.7 (2)	P(2)-Mo(2)-C(5)	96.0 (2)
P(3)-Mo(1)-P(5)	91.09 (5)	P(3)-Mo(2)-P(4)	62.33 (5)
P(3)-Mo(1)-O(1B)	124.71 (9)	P(3)-Mo(2)-C(3)	79.1 (2)
P(3)-Mo(1)-C(1)	72.9 (2)	P(3)-Mo(2)-C(4)	102.6 (2)
P(3)-Mo(1)-C(2)	91.7 (2)	P(3)-Mo(2)-C(5)	154.1 (2)
P(5)-Mo(1)-O(1B)	78.28 (9)	P(4)-Mo(2)-C(3)	95.1 (2)
P(5)-Mo(1)-C(1)	98.6 (2)	P(4)-Mo(2)-C(4)	163.9 (2)
P(5)-Mo(1)-C(2)	168.7 (2)	P(4)-Mo(2)-C(5)	102.0 (2)
O(1B)-Mo(1)-C(1)	161.9 (2)	C(3)-Mo(2)-C(4)	87.0 (3)
O(1B)-Mo(1)-C(2)	91.1 (2)	C(3)-Mo(2)-C(5)	82.2 (3)
C(1)-Mo(1)-C(2)	92.7 (2)	C(4)-Mo(2)-C(5)	94.1 (3)
Mo(1)-P(1)-O(11)	114.2 (2)	Mo(2)-P(2)-O(1B)	108.0 (1)
Mo(1)-P(1)-O(12)	119.7 (2)	Mo(2)-P(2)-O(4B)	110.5 (1)
Mo(1)-P(1)-O(13)	111.8 (2)	Mo(2)-P(3)-O(3B)	97.0 (1)
Mo(1)-P(3)-Mo(2)	82.02 (5)	Mo(2)-P(4)-O(2B)	114.1 (1)
Mo(1)-P(3)-O(3B)	115.1 (1)	Mo(2)-P(4)-O(3B)	96.5 (1)
Mo(1)-P(5)-O(2B)	114.0 (1)	O(11)-P(1)-O(12)	98.5 (3)
Mo(1)-P(5)-O(4B)	102.2 (1)	O(11)-P(1)-O(13)	106.0 (3)
Mo(1)-O(1B)-P(2)	99.6 (2)	O(12)-P(1)-O(13)	105.0 (3)
O(1B)-P(2)-O(4B)	101.9 (2)	O(2B)-P(5)-O(4B)	100.9 (2)
O(2B)-P(4)-O(3B)	98.7 (2)	P(4)-O(2B)-P(5)	119.8 (2)
P(3)-O(3B)-P(4)	101.7 (2)	P(2)-O(4B)-P(5)	108.9 (2)

[a] Estimated standard deviations are in parentheses.

45.2 (d, NC, J = 8.4, 10.4, 9.6, 9.2 Hz), 23.5–22.4 (m, Me). Anal. Calcd for $C_{34}H_{61}Mo_2N_5O_9P_4$ (**1e**): C, 40.85; H, 6.15; N, 7.01. Found: C, 40.87; H, 6.21; N, 6.75.

$Mo(CO)_3[^iPr_2NPO]_4Mo(CO)_3$ (1f). An amount of 0.66 g of complex **1e** was dissolved in 20 mL of toluene at 60 °C, and CO gas was bubbled through it for 6 h. The clear orange-red solution was evaporated to dryness and the residue chromatographed to give 0.31 g of complex **1f** (0.33 mmol, 50% yield). X-ray-quality crystals were grown from hexane solutions by slow evaporation. ^{1}H NMR: δ 3.92, 3.72 (m, NCH), 1.50 and 1.35 (d, Me, J = 6.7, 3.0 Hz), 1.31 (m, Me). ^{13}C NMR δ 220.8, 218.5, 217.6, 215.6, 208.0 (m, CO), 48.9, 48.2, 47.4, 45.3 (d, NC, J = 8.9, 10.3, 10.4, 8.6 Hz), 23.0 (m, Me). Anal. Calcd for $C_{30}H_{56}Mo_2N_4O_{10}P_4$ (**1f**): C, 37.99; H, 5.95; N, 5.91. Found: C, 37.57; H, 6.13; N, 5.71.

Table V. Selected Bond Distances (Å) and Angles (deg) for 1f[a]

Mo(1)-Mo(2)	3.143 (1)		
Mo(1)-P(1)	2.501 (3)	P(1)-O(2B)	1.599 (7)
Mo(1)-P(3)	2.403 (3)	P(1)-O(4B)	1.676 (7)
Mo(1)-O(1B)	2.265 (7)	P(2)---P(3)	2.544 (4)
Mo(1)-C(1)	1.94 (1)	P(2)-O(3B)	1.694 (7)
Mo(1)-C(2)	2.04 (1)	P(2)-O(4B)	1.621 (7)
Mo(1)-C(3)	2.03 (1)	P(3)-O(3B)	1.639 (7)
Mo(2)-P(2)	2.440 (3)	P(4)-O(1B)	1.526 (7)
Mo(2)-P(3)	2.443 (3)	P(4)-O(2B)	1.742 (8)
Mo(2)-P(4)	2.515 (3)	C(1)-O(1)	1.16 (1)
Mo(2)-C(4)	2.11 (2)	C(2)-O(2)	1.13 (1)
Mo(2)-C(5)	2.01 (1)	C(3)-O(3)	1.13 (1)
Mo(2)-C(6)	2.03 (1)	C(4)-O(4)	1.10 (2)
C(5)-O(5)	1.14 (1)	C(6)-O(6)	1.12 (1)
Mo(2)-Mo(1)-P(1)	78.42 (7)	Mo(1)-Mo(2)-P(2)	81.38 (7)
Mo(2)-Mo(1)-P(3)	50.11 (7)	Mo(1)-Mo(2)-P(3)	49.00 (7)
Mo(2)-Mo(1)-P(4)	49.01 (6)	Mo(1)-Mo(2)-P(4)	60.36 (7)
Mo(2)-Mo(1)-O(1B)	73.8 (2)	Mo(1)-Mo(2)-C(4)	125.2 (3)
P(1)-Mo(1)-P(3)	90.6 (1)	P(2)-Mo(2)-P(3)	62.8 (1)
P(1)-Mo(1)-O(1B)	79.2 (2)	P(2)-Mo(2)-P(4)	93.4 (1)
P(1)-Mo(1)-C(1)	97.5 (4)	P(2)-Mo(2)-C(4)	97.2 (1)
P(1)-Mo(1)-C(2)	91.6 (4)	P(2)-Mo(2)-C(5)	96.5 (4)
P(1)-Mo(1)-C(3)	167.7 (3)	P(2)-Mo(2)-C(6)	164.3 (4)
P(3)-Mo(1)-O(1B)	123.8 (2)	P(3)-Mo(2)-P(4)	107.0 (1)
P(3)-Mo(1)-C(1)	72.4 (3)	P(3)-Mo(2)-C(4)	81.5 (3)
P(3)-Mo(1)-C(2)	153.2 (4)	P(3)-Mo(2)-C(5)	151.8 (4)
P(3)-Mo(1)-C(3)	93.7 (3)	P(3)-Mo(2)-C(6)	103.7 (4)
O(1B)-Mo(1)-C(1)	163.2 (4)	P(4)-Mo(2)-C(4)	168.7 (4)
O(1B)-Mo(1)-C(2)	82.7 (4)	P(4)-Mo(2)-C(5)	92.4 (4)
O(1B)-Mo(1)-C(3)	88.8 (4)	P(4)-Mo(2)-C(6)	82.6 (4)
C(1)-Mo(1)-C(2)	80.9 (5)	C(4)-Mo(2)-C(5)	82.5 (5)
C(1)-Mo(1)-C(3)	94.8 (5)	C(4)-Mo(2)-C(6)	88.2 (5)
C(2)-Mo(1)-C(3)	89.8 (5)	C(5)-Mo(2)-C(6)	98.8 (5)
Mo(1)-P(1)-O(2B)	103.1 (3)	Mo(2)-P(2)-O(3B)	97.2 (3)
Mo(1)-P(1)-O(4B)	116.0 (3)	Mo(2)-P(2)-O(4B)	116.7 (3)
Mo(1)-P(3)-Mo(2)	80.89 (9)	Mo(2)-P(3)-O(3B)	98.6 (3)
Mo(1)-P(3)-O(3B)	113.1 (3)	Mo(2)-P(4)-O(1B)	108.0 (3)
Mo(1)-O(1B)-P(4)	97.7 (4)	Mo(2)-P(4)-O(2B)	110.5 (3)
O(1B)-P(4)-O(2B)	103.3 (4)	P(1)-O(2B)-P(4)	107.9 (4)
P(2)-O(3B)-P(3)	99.5 (4)	P(1)-O(4B)-P(2)	116.5 (4)
O(2B)-P(1)-O(4B)	100.3 (4)	O(3B)-P(2)-O(4B)	98.0 (4)

[a] Estimated standard deviations are in parentheses.

X-ray Structural Determination of Complex 1d. A summary of crystal data, data collection, and structural refinement details is presented in Table III. The intensities of a 0.6- × 0.4- × 0.7-mm crystal were collected on a Rigaku AFC6S diffractometer. A total of 11384 unique reflections were measured of which 6070 were considered significant at the 3σ level. The structure was solved using direct methods, and hydrogens were included at calculated positions.[15] Final least squares were performed varying 497 parameters. Final R_F = 0.042 and R_w = 0.044 with a goodness-of-fit (GOF) of 1.32. Selected bond distances and angles are listed in Table IV. Full atomic coordinates as well as anisotropic temperature factors plus structure factor tables are included in the supplementary material.

X-ray Structural Determination of Complex 1f. A summary of crystal data, data collection, and structural refinement details is presented in Table III. The intensities of a 1.0- × 1.0- × 1.0-mm crystal were collected to yield a total of 11150 unique reflections of which 4723 were considered significant at the 3σ level. The structure was solved using direct methods, and the

(15) Gilmore, C. J. MITHRIL. *J. Appl. Cryst.* **1984**, *17*, 42. Beurskens, P. T. DIRDIF. Technical Report 1984/1; Crystallography Laboratory: Toernooiveld, 6525 Ed Nijmegen, Netherlands, 1984.

non-hydrogen atoms were refined anisotropically.[15] Final least squares were performed using 452 variables. Final $R_f = 0.054$ and $R_w = 0.074$ with a GOF of 2.00. Selected bond distances and angles are presented in Table V. Complete atomic coordinates and anisotropic thermal factors as well as structure factor tables are included in the supplementary material.

Acknowledgment. We are grateful to the donors of the Petroleum Research Fund, administered by the American Chemical Society, for financial support. We also thank the National Science Foundation for an instrument grant to Keene State College for establishing a Molecular Structural Center and Professor R. Butcher of Howard University for helpful discussions.

Registry No. **1a**, 139409-20-4; **1b**, 139409-21-5; **1c**, 139409-22-6; **1d**, 139409-27-1; **1e**, 139409-28-2; **1f**, 139409-29-3; **2** (equatorial isomer), 139409-25-9; **2** (axial isomer), 139492-54-9; **3** (equatorial/equatorial isomer), 139409-26-0; **3** (equatorial/axial isomer 1), 139492-55-0; **3** (equatorial/axial isomer 2), 139492-56-1; **3** (axial/axial isomer), 139492-57-2; **4**, 139409-23-7; **5**, 139409-24-8; Mo, 7439-98-7; $Mo(CO)_4[^iPr_2NPO]_4Mo(CO)_4$, 88008-34-8.

Supplementary Material Available: Figures showing two-dimensional COSY ^{31}P NMR spectra of complexes **2** and **3** and tables of atomic coordinates, bond angles and distances, and isotropic and anisotropic thermal parameters for **1d** and **1f** (24 pages); tables of observed and calculated structure factors (148 pages). Ordering information is given on any current masthead page.

Preparation and NMR Studies of Hexacoordinated Fluorosilicates: Nondissociative Fluorine Site Exchange within the Octahedral Complexes in Solution

Claire Brelière, Francis Carré, Robert J. P. Corriu,* William E. Douglas, Monique Poirier, Gérard Royo, and Michel Wong Chi Man

Laboratoire "Hétérochimie et Amino-acides", CNRS, URA 1097, Université de Montpellier II, Sciences et Techniques du Languedoc, Place E. Bataillon, 34095 Montpellier Cedex 5, France

Received July 16, 1991

Stable 18-crown-6 potassium salts of hexacoordinated tetrafluorosilicates were readily prepared from pentacoordinated trifluorosilanes by reaction with KF/18-crown-6. It also proved possible to perform this transformation even in the absence of 18-crown-6. The crystal structure of the 18-crown-6 potassium salt of (8-(dimethylamino)naphthyl)tetrafluorosilicate was determined and the complex was found to exhibit slightly distorted octahedral geometry. Interestingly, the coordinative Si–N bond is shorter in this hexacoordinated complex (2.213 Å) than in the corresponding pentacoordinated one (2.318 Å). The results of solution NMR studies are consistent with the structure being octahedral. They indicate that intramolecular permutation of fluorine atoms occurs through a regular mechanism, such as the Bailar twist, without cleavage of either the Si–N or Si–F bonds. Similarly, a compound containing two hexacoordinated silicon atoms in the same molecule was prepared. Both silicons were found to be equivalent with fluorine site exchange occurring via a regular mechanism.

Introduction

Both penta- and hexacoordinated silicon compounds have received much attention in recent years. Most of the anionic complexes known have been obtained with exclusively electronegative groups bound directly to silicon,[1] and only a few hexacoordinated neutral or anionic species with more than one carbon–silicon bond have been described.[2] Possible applications for the organopentafluorosilanes are as reagents in organic synthesis,[3,4] and for the silicon tris(catecholates) as intermediates in the direct preparation of silanes from silica.[5]

The hexa- and pentafluorosilicate ions, SiF_6^- and $RSiF_5^-$ (R = alkyl or aryl group) were reported long ago as being air-stable compounds easily isolated in the pure state.[1b,2a] The structure of $2M^+,SiF_6^-$ (M: K^+, Na^+, NH_4^+) has been found to be based on a distorted octahedron.[1a,6]

Recently, Damrauer and Danahey described a general procedure for the preparation of pentacoordinated fluorosilicates in nonpolar solvents using KF solubilized by 18-crown-6.[7] The F^- ion released reacts with neutral tetracoordinated silicon compounds. The method has been applied to the preparation of a wide variety of pentacoordinated fluorosilicates.[8]

(1) (a) Tandura, S. N.; Voronkov, M. G.; Alekseev, N. V. *Top. Curr. Chem.* **1986**, *131*, 99. (b) Corriu, R. J. P.; Young, J. C. In *The Chemistry of Organic Silicon Compounds*; Patai, S., Rappoport, Z., Eds.; Wiley: Chichester, U.K., 1989; pp 1241–1288 (see also references therein). (c) Marat, R. K.; Jantsen, A. F. *J. Chem. Soc., Chem. Commun.* **1977**, 671. (d) Kummer, D.; Chaudhry, S. C.; Debaerdemaeker, T.; Thewalt, U. *Chem. Ber.* **1990**, *123*, 945. (e) Holmes, R. R. *Chem. Rev.* **1990**, *90*, 17.

(2) (a) Farnham, W. B.; Whitney, J. F. *J. Am. Chem. Soc.* **1984**, *106*, 3992. (b) Brelière, C.; Carré, F.; Corriu, R. J. P.; Poirier, M.; Royo, G.; Zwecker, J. *Organometallics* **1989**, *8*, 1831. (c) Taba, K. M.; Dahloff, W. V. *J. Organomet. Chem.* **1985**, *280*, 27. (d) Müller, R. *Z. Chem.* **1965**, *5*, 220.

(3) Müller, R. *Z. Chem.* **1984**, *24*, 41.

(4) (a) Kumada, M.; Tamao, K.; Yoshida, J. I. *J. Organomet. Chem.* **1982**, *239*, 115. (b) Tamao, K.; Toshida, J.; Yamamoto, H.; Kakui, T.; Yatsumoto, H.; Takahashi, M.; Kurita, A.; Murata, M.; Kumada, M. *Organometallics* **1982**, *1*, 335. (c) Tamao, K.; Kakui, T.; Akita, M.; Iwahara, T.; Kanatani, R.; Yoshida, J.; Kumada, M. *Tetrahedron* **1983**, *9*, 983.

(5) Boudin, A.; Cerveau, G.; Chuit, C.; Corriu, R. J. P.; Reyé, C. *Angew. Chem., Int. Ed. Engl.* **1986**, *25*, 474; *Organometallics* **1989**, *7*, 1165.

(6) Ketelaar, J. A. A. *Kristallografiya* **1935**, *92*, 155.

(7) Damrauer, R.; Danahey, S. E. *Organometallics* **1986**, *5*, 1490.

(8) (a) Damrauer, R.; O'Connell, B.; Danahey, S. E.; Simon, R. *Organometallics* **1989**, *8*, 1167. (b) Brefort, J. L.; Corriu, R. J. P.; Guérin, C.; Henner, B. H. L.; Wong Chi Man, W. W. C. *Organometallics* **1990**, *9*, 2080. (c) Day, R. O.; Sreelatha, C.; Deiters, J. A.; Johnson, S. E.; Holmes, J. M.; Howe, L.; Holmes, H. H. *Organometallics* **1991**, *10*, 1758. (d) Johnson, S. E.; Day, R. O.; Holmes, R. R. *Inorg. Chem.* **1989**, *28*, 3182. (e) Johnson, S. E.; Payne, J. S.; Day, R. O.; Holmes, J. M.; Holmes, R. R. *Inorg. Chem.* **1989**, *28*, 3190.

0276-7333/92/2311-1586$03.00/0